

# 4-Methyl-1-(prop-2-yn-1-yl)-1H-1,2,3-triazole (MPT): A Novel, Highly Efficient Nitrification Inhibitor for Agricultural Applications

Sibel C. Yildirim, Joses G. Nathanael, Katharina Frindte, Otávio dos Anjos Leal, Robert M. Walker, Ute Roessner, Claudia Knief, Nicolas Brüggemann, and Uta Wille\*



Cite This: *ACS Agric. Sci. Technol.* 2024, 4, 255–265



Read Online

ACCESS |



Metrics & More



Article Recommendations



Supporting Information

**ABSTRACT:** Nitrogen fertilization in agriculture has serious environmental consequences, including production of the greenhouse gas nitrous oxide ( $\text{N}_2\text{O}$ ), pollution of groundwater with nitrate ( $\text{NO}_3^-$ ), and river eutrophication. Nitrogen use efficiency can be increased by amending fertilizers with inhibitors to slow microbial nitrification processes, which transform ammonia to  $\text{NO}_3^-$ . Unfortunately, commercial inhibitors have failed to perform reliably across various agroecosystems for reasons not well understood. Using a combination of bacterial studies and soil incubations, we demonstrate here that 4-methyl-1-(prop-2-yn-1-yl)-1H-1,2,3-triazole (MPT) exhibits superior nitrification inhibitory properties. Unlike the commercial reversible inhibitors, MPT acts as a mechanistic, irreversible inhibitor of the key enzyme ammonia monooxygenase, enabling effective retention of ammonium ( $\text{NH}_4^+$ ) and suppression of  $\text{NO}_3^-$  and  $\text{N}_2\text{O}$  production over 21 days in several agricultural soils with pH values ranging from 4.7 to 7.5. A bacterial viability stain and a suite of freshwater and terrestrial ecotoxicity tests did not indicate any acute or chronic toxicity. Real-time quantitative polymerase chain reaction (qPCR) analysis revealed an enhanced inhibitory effect of MPT on both ammonia-oxidizing bacteria and archaea. Thus, MPT outperforms currently available nitrification inhibitors and has great potential for broad application in various agricultural settings.

**KEYWORDS:** ammonia monooxygenase, bacterial assay, greenhouse gas emissions, inhibition mechanism, nitrification, nitrification inhibitor, soil incubations

## INTRODUCTION

Providing food for the constantly growing population will require a 70–100% increase in nitrogen (N) fertilizer usage worldwide by 2050, which is exacerbated by limited arable land and deteriorating agricultural conditions, particularly due to global warming.<sup>1</sup> Unfortunately, since several decades, N use efficiency (NUE) has remained at only around 50% globally.<sup>2–4</sup> A large fraction of N fertilizers is lost from agricultural systems, for example, through volatilization of ammonia ( $\text{NH}_3$ ), a precursor of fine particulate matter ( $\text{PM}_{2.5}$ ), and nitrate ( $\text{NO}_3^-$ ) leaching, which causes surface water eutrophication and groundwater pollution.<sup>2,5–7</sup> Microbial nitrification and denitrification processes lead to the formation of the gases nitrous oxide ( $\text{N}_2\text{O}$ ), nitric oxide (NO), and nitrogen ( $\text{N}_2$ ).<sup>8</sup>  $\text{N}_2\text{O}$  has a 300 times higher global warming potential than carbon dioxide, and reduction of N losses has become an important goal to lowering agriculture's greenhouse gas footprint.<sup>7</sup>

One strategy to improve N management in agricultural soils is by amending N fertilizers with nitrification inhibitors (NIs).<sup>9,10</sup> Nitrification is carried out by ammonia-oxidizing bacteria (AOB) and archaea (AOA). NIs are intended to inhibit the transmembrane enzyme ammonia monooxygenase (AMO),<sup>11–13</sup> which catalyzes the rate-limiting first oxidation step of  $\text{NH}_3$  to hydroxylamine ( $\text{NH}_2\text{OH}$ ).<sup>14,15</sup>  $\text{NH}_2\text{OH}$  is subsequently converted via NO to nitrite ( $\text{NO}_2^-$ ) mediated by hydroxylamine oxidoreductase (HAO), followed by rapid oxidation to  $\text{NO}_3^-$ , the end-product of nitrification catalyzed

by nitrite oxidase.<sup>16–19</sup> Some strains of *Nitrospira* (complete ammonia oxidizers, comammox) can catalyze the complete oxidation from  $\text{NH}_3$  to  $\text{NO}_3^-$ , also initiated by AMO.<sup>20</sup> Thus, inhibition of AMO should increase the residence time of  $\text{NH}_3$  (or ammonium,  $\text{NH}_4^+$ ) and reduce N losses from soil through  $\text{NO}_3^-$  leaching and  $\text{N}_2\text{O}$  emissions.

While many NIs are known,<sup>14</sup> only three are currently commercially available: 3,4-dimethyl-1H-pyrazole (DMP), which is commonly applied as the salt of phosphoric acid (DMPP or ENTEC, BASF AG)<sup>21</sup> or glycolic acid (DMPG or eNpower, Incitec Pivot Fertilisers), dicyandiamide (DCD, AlzChem AG), and 2-chloro-6-(trichloromethyl)pyridine (Nitrapyrin or N-Serve, Dow Chemical Co.) (Figure 1a). However, these come with certain limitations and are, therefore, not generally applied.

Various field studies in neutral soils showed an unreliable efficacy of DMP in improving crop yields.<sup>22–25</sup> In acidic soils and dry climates, the already only moderate nitrification inhibitory effect decreased even further with increasing temperature from 45% (10 °C) to just 23% (25 °C).<sup>26,27</sup> Even more concerning are results from field studies in hot-dry

**Received:** November 12, 2023

**Revised:** January 14, 2024

**Accepted:** January 18, 2024

**Published:** February 1, 2024



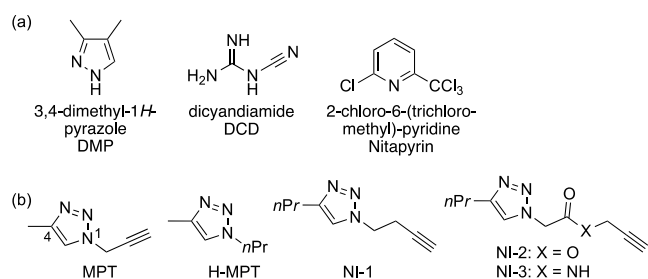


**Figure 1.** (a) Commercial nitrification inhibitors. (b) Substituted 1,2,3-triazoles studied in this work.

climates of Australia where essentially no inhibitory effect of DMP was found.<sup>26,28,29</sup> DCD has been shown to be ten times less effective than DMP,<sup>30</sup> with its performance depending on temperature.<sup>31</sup> Furthermore, due to its water-solubility, DCD can leach into groundwater and has been detected in dairy products in New Zealand, resulting in its government stopping the sale of milk products containing DCD.<sup>32,33</sup> Nitrapyrin is comparatively volatile and only sparingly water-soluble<sup>34</sup> and has been identified as an air pollutant.<sup>35</sup> It has shown bactericidal properties, considerable acute and chronic aquatic toxicity, and is currently banned in some countries.<sup>35</sup> Thus, in light of the inconsistent performance of the commercial NIs,<sup>23,27,36–38</sup> particularly in acidic soils,<sup>38–40</sup> it is remarkable that since the discovery of DMPP more than 20 years ago,<sup>21</sup> no new inhibitor compounds have been developed and brought to market that offer improved efficiency and effectiveness in slowing down the nitrification process. A better control of N availability for crops, increased crop yield, and improved quality is essential for meeting the growing global demand for food while minimizing the environmental impact of N fertilization in agriculture.

Unfortunately, the structure of AMO is not yet known. On the contrary, the recently crystallized particulate methane monooxygenase (pMMO), which is evolutionally comparable with AMO, suggests that a cupredoxin-like unit could be involved in the oxidation of  $\text{NH}_3$ .<sup>41–43</sup> We recently showed that DMP and DCD are uncompetitive and reversible AMO inhibitors, suggesting that their unreliable performance might be, at least to some extent, due their nonmechanistic mode of inhibition, for example, by chelating metal centers in the active site.<sup>30,41–44</sup> To effectively increase the NUE of N-fertilization, we are postulating that “successful” NIs should inhibit AMO irreversibly (i.e., mechanism-based inhibitors). Recovery of the activity of nitrifying bacteria would require the *de novo* synthesis of the enzyme. Examples for mechanism-based NIs are acetylene and phenylacetylene,<sup>45–47</sup> but their volatility, high flammability, or environmental toxicity prohibit their use in agriculture. Thus, irreversible NIs for field applications are at present not available.

Recently, we have presented substituted 1,2,3-triazoles as a promising new class of NIs.<sup>48</sup> 1,2,3-Triazoles are readily synthetically available with a large substituent variability and provide an excellent scaffold for terminal alkyne chains, thereby combining the metal chelating property of the N-heterocyclic ring with the chemical reactivity of acetylene. We demonstrate here that 4-methyl-1-(prop-2-yn-1-yl)-1H-1,2,3-triazole (MPT, Figure 1b) represents a novel mechanistic and irreversible inhibitor of AMO, as revealed by *in vitro* bacterial assays. Soil incubations showed that MPT exhibits outstanding inhibitory qualities by effectively retaining  $\text{NH}_4^+$  and

suppressing  $\text{NO}_3^-$  formation and  $\text{N}_2\text{O}$  emissions over a period of 21 days, particularly in acidic soils, where the current commercial NIs often fail to perform.

## MATERIALS AND METHODS

**Chemicals.** DMP (3,4-dimethyl-1H-pyrazole) was supplied by Incitec Pivot Fertilisers Australia. *Nitrosomonas europaea* (*N. europaea*; ATCC19718) was purchased from the American Type Culture Collection. *Nitrosospora multiformis* (*N. multiformis*) was isolated from an aquarium kit as described previously.<sup>49</sup> 4-Methyl-1-(prop-2-yn-1-yl)-1H-1,2,3-triazole (MPT; molecular weight: 121.07 g mol<sup>-1</sup>) and 4-methyl-1-propyl-1H-1,2,3-triazole (H-MPT; molecular weight: 125.10 g mol<sup>-1</sup>) were synthesized according to the procedure reported by Clark et al.<sup>50</sup> 1-(3-Butyn-1-yl)-4-propyl-1H-1,2,3-triazole (NI-1; molecular weight: 163.22 g mol<sup>-1</sup>), prop-2-yn-1-yl 2-(4-propyl-1H-1,2,3-triazol-1-yl)acetate (NI-2; molecular weight: 207.23 g mol<sup>-1</sup>), and prop-2-yn-1-yl 2-(4-propyl-1H-1,2,3-triazol-1-yl)-acetamide (NI-3; molecular weight: 206.24 g mol<sup>-1</sup>) were provided by Taggart et al. and were synthesized as described.<sup>48</sup> Synthetic details and spectroscopic data are provided in the Supporting Information.

**Studies with AOB.** The growth and harvest of pure bacterial cell cultures of *N. europaea* and *N. multiformis*, the standard activity and activity recovery assays, the measurements of the  $\text{O}_2$  consumption, Michaelis–Menten kinetics, and acute toxicity tests were conducted as previously reported.<sup>30,49,51</sup> All bacterial incubations were performed in sodium phosphate buffer (NaPB) with 1% (v/v) DMSO at pH = 7.5 and 30 °C with different inhibitors and concentrations, as indicated. This amount of DMSO, which was required to solubilize the lipophilic inhibitor compounds, is not detrimental to the bacterial cells.<sup>49</sup> Experimental details are provided in the Supporting Information.

**Mineral-N Transformation Studies.**<sup>48</sup> Soil incubations to determine the loss of  $\text{NH}_4^+$  and production of  $\text{NO}_3^-$  over 21 days after treatment were performed in an Australian soil (soil A; pH = 5.9, see Table S9 for soil specifications). Treatments were: (1) fertilizer only ( $(\text{NH}_4)_2\text{SO}_4$ , 100 mg N kg<sup>-1</sup> soil), (2) fertilizer + 0.5 mol % MPT, (3) fertilizer + 2.5 mol % MPT, (4) fertilizer + 5 mol % MPT, and (5) fertilizer + 5 mol % DMP, with three replicates of each treatment per time interval. Detailed data are given in the Supporting Information.

**$\text{N}_2\text{O}$  Measurements.**<sup>52,53</sup> Soil incubations were performed with four German soils (soils B–E) with varying pH values (soil specifications are provided in Table S9). Each of the three replicates consisted of 6 g of sieved soil (2 mm). The soil was air-dried after collection and preincubated prior to the experiment for 7 days at 50% water holding capacity (WHC). The soil was transferred to a gas chromatography vial (22 mL volume, clear glass, Macherey-Nagel, Germany) and compacted densely to allow 5.5–6.2 cm headspace. The soil in the vials was incubated for a total of 21 days at a constant temperature of 21 °C with an open lid to ensure gas circulation. The control incubations contained “untreated” soil (deionized  $\text{H}_2\text{O}$  only) and “fertilizer only” soil ( $(\text{NH}_4)_2\text{SO}_4$ ; 50 mg kg<sup>-1</sup> soil) and accompanied each measurement.  $(\text{NH}_4)_2\text{SO}_4$  was applied as an aqueous solution (1 g  $\text{NH}_4^+$  mL<sup>-1</sup>  $\text{H}_2\text{O}$ ) and introduced on the soil surface to mimic field conditions. Three inhibitor solutions were prepared from DMP and MPT at concentrations of 0.5 mol %, 2.5 mol %, and 5 mol % of applied fertilizer-N (see Table S10) and applied on the soil surface. The soils reached 60% WHC after the treatments had been applied and were kept at that moisture level by periodically adding deionized water to compensate for the evaporation losses.

At the day of measurement (days 1, 3, 5, 7, 14, and 21 after fertilization), the vials were closed gastight with a rubber septum and aluminum lid and opened again after each measurement. The  $\text{N}_2\text{O}$  emission was analyzed using a gas chromatograph equipped with an electron capture detector and a flame ionization detector (GC-ECD/FID; Clarus 580, PerkinElmer). Details of the calculation of the  $\text{N}_2\text{O}$  production rate are provided in the Supporting Information.

**Real-Time Quantitative Polymerase Chain Reaction (qPCR) Analysis of Bacterial and Archaeal *amoA*.** Soil samples (400 mg) from the N<sub>2</sub>O experiments after the 21-day incubation period were used to extract DNA using a NucleoSpin Soil DNA extraction kit (Macherey Nagel, Germany) according to the manufacturer's instruction. For the extraction, the SL1 buffer and enhancer were chosen, and DNA was finally eluted in 40  $\mu$ L of PCR-grade water. Real-time qPCR of *amoA* genes was performed for the bacterial and archaeal community for each treatment with three biological and three technical replicates. The primers Arch-*amoA*F and Arch-*amoA*R were used for AOA,<sup>54</sup> while *amoA*-1F and *amoA*-2R were used for AOB.<sup>55</sup> The DNA extracts were diluted 10-fold to avoid inhibitory effects. Real-time qPCR assays were performed on a Bio-Rad CFX Connect real-time PCR machine. The quantification was performed using 5.0  $\mu$ L of SYBR Green Master Mix (BioRad, USA), 0.4  $\mu$ L of the forward and reverse primer (10 pmol  $\mu$ L<sup>-1</sup>), 3.2  $\mu$ L of PCR-H<sub>2</sub>O, and 1  $\mu$ L of the 10-fold diluted DNA. The fragments of bacterial and archaeal *amoA* genes were amplified using an initial denaturation phase (2 min), followed by 40 cycles (i) at 95 °C (10 s), (ii) annealing at 72 °C for bacteria (1 min) and archaea (30 s), and (iii) elongation for 45 s at 57.4 °C (bacteria) and 60 °C (archaea). The PCR reaction runs had an efficiency between 97 and 111%. Standard curves were generated using serial dilutions ranging from 10<sup>8</sup> to 10<sup>3</sup> gene copies per reaction, provided as linearized plasmids that contained cloned *amoA* genes of bacteria or archaea ( $R^2 > 0.8$ ). The correct PCR product length was verified by obtaining a melting curve in the temperature range 65–95 °C.

**Statistical Analysis.** Statistical analysis was performed with three technical (except for the GC studies) and three biological replicates. For the bacterial cell studies, NO<sub>2</sub><sup>-</sup> production,  $K_{m(app)}$ ,  $V_{max(app)}$ , and  $k_{obs}$  values for inhibited and uninhibited cells were determined using Student's *t* test with a significance level of  $p < 0.05$  using GraphPad Prism version 9.5.0. Statistical analysis for the NH<sub>4</sub><sup>+</sup> and NO<sub>3</sub><sup>-</sup> measurements and the N<sub>2</sub>O production rates were performed with GraphPad Prism 9.5.0 via two-way analysis of variance (2-way ANOVA), assessing the factors day and treatment at each time point using the Tukey HSD posthoc test with a significance level of  $p < 0.05$ . Statistical analyses on gene copy numbers were performed with GraphPad Prism 9.5.0 (ordinary one-way ANOVA) with GraphPad Prism 9.5.0 (2-way ANOVA) multiple comparison Tukey HSD. All results are reported as mean values  $\pm$  standard error of the mean.

## RESULTS AND DISCUSSION

**Structure–Activity Relationship (SAR) Studies.** Figure 1b shows the substituted 1,2,3-triazoles ("inhibitors") studied in this work, which were designed to assess the role of the alkyne moiety and its position relative to the triazole ring on the inhibitory activity. Bacterial studies were performed using pure cultures of nitrifying bacteria *N. europaea* and *N. multiformis*. The cultures were incubated with ammonium sulfate ((NH<sub>4</sub>)<sub>2</sub>SO<sub>4</sub>), and the production of NO<sub>2</sub><sup>-</sup> measured after 60 min in an assay based on the Griess reaction developed recently by us (see the Supporting Information for details).<sup>49</sup>

Table 1 shows that the activity of both *N. europaea* and *N. multiformis* cells dropped to about 25% upon treatment with MPT, compared with the uninhibited cells, revealing an excellent inhibitory activity of this compound. Interestingly, H-MPT, which has a propyl instead of the propargyl substituent, had no impact on the activity of both cultures, clearly demonstrating the importance of the alkyne moiety in MPT for enzyme inhibition. On the contrary, NI-1, which has a propyl group at C-4 and a butynyl instead of a propynyl chain, reduced the activity to an average of about 70% in both cultures. The alkynyl ester in NI-2 lowered the enzyme activity to about 50%, whereas the alkynyl amide substituent in NI-3 almost eradicated any inhibitory effect.

**Table 1. Percent Activity of *N. europaea* and *N. multiformis* after Treatment with Various 1,4-Disubstituted 1,2,3-Triazoles, Determined from the NO<sub>2</sub><sup>-</sup> Production<sup>a</sup>**

inhibitor	% activity	
	<i>N. europaea</i>	<i>N. multiformis</i>
MPT	24 $\pm$ 5	25 $\pm$ 4
H-MPT	100	100
NI-1	79 $\pm$ 2	60 $\pm$ 1
NI-2	51 $\pm$ 2	53 $\pm$ 2
NI-3	93 $\pm$ 1	100

<sup>a</sup>Incubations were performed in NaPB (pH = 7.5) with 1% (v/v) DMSO at 30 °C with [NH<sub>4</sub><sup>+</sup>] = 3 mM and [inhibitor] = 0.3 mM (10 mol % of N-source) at 100 rpm for 60 min in the dark. Standard errors were determined from three biological replicates (see Tables S1 and S2 for complete data). The percent activity was calculated according to eq SI-1.<sup>49</sup>

These SAR data show a strong dependence of the enzyme's activity on the substitution pattern, in particular, the position of the alkyne moiety relative to the triazole ring. Additional factors, such as size, polarity, or hydrogen-bonding abilities, are also obviously influencing the inhibitory activity, which will be explored in more detail in future work by us.

**Reversible or Irreversible Inhibition?** The three best performing compounds from the SAR experiments, i.e., MPT, NI-1, and NI-2, were subsequently explored for their reversibility of AMO inhibition. Cells of *N. europaea* and *N. multiformis* were incubated for 30 min with NH<sub>4</sub><sup>+</sup> and the inhibitors MPT, NI-1, and NI-2, and NO<sub>2</sub><sup>-</sup> production was measured (a high inhibitor loading of 50 mol % of the applied NH<sub>4</sub><sup>+</sup> was chosen to ensure noticeable effects). The cells were subsequently washed thoroughly with NaPB to remove any unbound and bound inhibitor compound, followed by reincubation with NH<sub>4</sub><sup>+</sup> for 30 min and measurement of the NO<sub>2</sub><sup>-</sup> production. Reversible binding of the NI to AMO would be expected to result in a recovery of the NO<sub>2</sub><sup>-</sup> production activity after washing and reincubation, approximately to the level of the uninhibited cells, as we have recently found for DMP, DCD, and a series of 1,4-disubstituted 1,2,3-triazoles.<sup>30,51</sup> Control experiments in the absence of inhibitor confirmed that the washing and reincubation protocol did not impact (within error) the NO<sub>2</sub><sup>-</sup> production rate of both bacterial strains.

Before washing, treatment with MPT reduced NO<sub>2</sub><sup>-</sup> production substantially compared to the uninhibited cells, irrespective of the AMO orthologue (Table 2), confirming the findings from the SAR studies shown in Table 1.

Most importantly, after washing the MPT-treated cells and reincubation with NH<sub>4</sub><sup>+</sup>, the activity did not increase significantly ( $p > 0.05$ ), clearly showing that MPT irreversibly inhibits AMO. Recovery of the full NO<sub>2</sub><sup>-</sup> production rate requires *de novo* synthesis of AMO, which has been shown to take at least several hours, depending on the duration of exposure to the inhibitor.<sup>46,56</sup> In contrast, compounds NI-1 and NI-2 are reversible inhibitors, leading to a recovery of activity after washing and reincubation, which shows that the presence of an alkyne substituent does not necessarily lead to irreversible inhibition.

From these experiments, MPT has emerged as both the best-performing and exclusive irreversible inhibitor. In the following, the mechanism of inhibition and the inhibitory performance of MPT in different soils are further explored.

**Table 2. Recovery of NO<sub>2</sub><sup>-</sup> Production by Pure Cell Cultures of *N. europaea* and *N. multiformis* After Treatment with Alkynyl-Substituted 1,2,3-Triazoles<sup>a</sup>**

AMO source	inhibitor	NO <sub>2</sub> <sup>-</sup> production/nmol L <sup>-1</sup> min <sup>-1</sup>	
		before washing	after washing
<i>N. europaea</i>		1537 ± 512	1458 ± 255
<i>N. europaea</i>	MPT	379 ± 51	317 ± 73
<i>N. multiformis</i>		1314 ± 374	1777 ± 293
<i>N. multiformis</i>	MPT	345 ± 77	358 ± 39
<i>N. multiformis</i>	NI-1	487 ± 82	944 ± 53
<i>N. multiformis</i>	NI-2	796 ± 14	1482 ± 42

<sup>a</sup>NO<sub>2</sub><sup>-</sup> production rates were determined in the presence of NIs and after repeated washing with NaPB and subsequent re-incubation with NH<sub>4</sub><sup>+</sup>. The incubations were performed in NaPB (pH = 7.5) and 1% (v/v) DMSO with [NH<sub>4</sub><sup>+</sup>] = 3.0 mM and [inhibitor] = 1.5 mM at 30 °C and 100 rpm in the dark. Standard errors were calculated from three biological replicates, each performed with three technical replicates.

**Identifying the Enzyme Targeted by MPT.** As outlined in the introduction, the first two steps of the oxidation of NH<sub>3</sub> to NO<sub>3</sub><sup>-</sup>, i.e., NH<sub>3</sub> → NH<sub>2</sub>OH → NO<sub>2</sub><sup>-</sup> (via NO) are catalyzed by the enzymes AMO and HAO, respectively. As our bacterial assay is based on measuring the production of NO<sub>2</sub><sup>-</sup>, either of these two enzymes could principally be targeted by MPT. The finding that MPT reduced the NO<sub>2</sub><sup>-</sup> production of cell cultures supplemented with NH<sub>4</sub><sup>+</sup> to about one-quarter (Table 1) suggests that this inhibitor blocks AMO. To confirm the selectivity for AMO, a separate experiment was performed where *N. europaea* and *N. multiformis* cultures were treated with NH<sub>2</sub>OH as substrate for HAO and the production of NO<sub>2</sub><sup>-</sup> measured after 60 min. Interestingly, a reduction of the activity of both bacterial cell cultures of about 30% was found (Table S3), which suggests that MPT might inhibit also HAO. However, AMO and HAO are not independently operating enzymes but are interconnected through an electron shuttle mechanism.<sup>57</sup> Thus, disruption of the electron transfer chain due to strong AMO inhibition by MPT should also lead to (partial) inhibition of HAO, similar to what has been previously found for the AMO inhibitors DMP and hydrazine.<sup>30,58</sup>

**Measurement of the Oxygen (O<sub>2</sub>) Consumption.** As the rate of O<sub>2</sub> uptake by AMO is proportional to the oxidation of NH<sub>3</sub> to NH<sub>2</sub>OH,<sup>57</sup> exploration of the kinetics of O<sub>2</sub> consumption in the presence of MPT enables to obtain insight into the mechanism of enzyme inhibition. Real-time kinetic measurements were performed with cell suspensions of *N. europaea* at 20 °C using a Clark-type oxygen electrode, where the decrease of [O<sub>2</sub>] in the presence of NH<sub>4</sub><sup>+</sup> was first monitored for 5 min. MPT was then added; the system was equilibrated for 15 s, and the O<sub>2</sub> decay was subsequently measured for a further 5 min. [MPT] was chosen such that the uptake of the O<sub>2</sub> by AMO was not completely stopped. In all measurements, both NH<sub>4</sub><sup>+</sup> and O<sub>2</sub> were present in excess so that the O<sub>2</sub> uptake rate was only dependent on the enzyme concentration (the total protein concentration was ca. 468 μg L<sup>-1</sup>, determined via a BCA assay kit). Thus, the O<sub>2</sub> consumption by uninhibited cells should follow zero order kinetics. Figure 2 shows the time-dependent [O<sub>2</sub>] profile before and after treatment of the cells with 0.6 and 1.2 mM MPT, respectively.

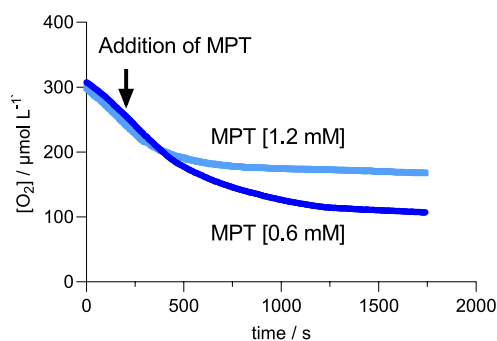


**Figure 2.** Time-dependent O<sub>2</sub> consumption by *N. europaea* in the absence and presence of MPT. The first 240 s show the consumption of the O<sub>2</sub> in the absence of MPT. After 255 s, MPT was added (indicated by the arrow); [MPT] = 0.6 mM (dark blue trace) and 1.2 mM (light blue trace). The cells were treated with [NH<sub>4</sub><sup>+</sup>] = 3.0 mM in NaPB (pH = 7.5) with 1% (v/v) DMSO at 20 °C under constant stirring in the dark. The plot shows the mean of three measurements for each MPT concentration; standard errors have been omitted for clarity and are reflected by the rate coefficient, *k*, for the uninhibited cells.

Addition of MPT considerably slowed the consumption of O<sub>2</sub> by *N. europaea*. While the uninhibited cells showed, as expected, zero order kinetics with an average rate coefficient of  $k = 275 \pm 20 \text{ nmol O}_2 \text{ L}^{-1} \text{ s}^{-1}$  (Figure S1 and Table S4), the decay profile after the addition of MPT changed to follow first order kinetics, yielding rate coefficients for the O<sub>2</sub> consumption of  $k = (2.8 \pm 1.3) \times 10^{-3} \text{ s}^{-1}$  and  $(4.8 \pm 1.4) \times 10^{-3} \text{ s}^{-1}$  for [MPT] = 0.6 mM and 1.2 mM, respectively (Figure S2 and Table S5).

As the rate of O<sub>2</sub> consumption in the presence of MPT is a measure for the rate of enzyme inhibition, the observed rate increase with increasing [MPT] (doubling [MPT] increased the rate of inhibition by a factor of about two), is indicative for a mechanistic inhibition, where the amount of active enzymes declines over time, similar to what has previously been reported for acetylene and phenylacetylene.<sup>45,47</sup> These data confirm that MPT inhibits AMO through a chemical reaction, likely through the formation of covalent bonds, in alignment with our design rationale outlined in the introduction.

**Michaelis–Menten Kinetics.** To gain insight into the binding site of MPT in AMO, Michaelis–Menten kinetics were studied by measuring the production of NO<sub>2</sub><sup>-</sup> by *N. europaea* at various [NH<sub>4</sub><sup>+</sup>] and constant [MPT]. Figure 3 shows the formation of NO<sub>2</sub><sup>-</sup> by uninhibited cells and cells treated with 37.5 and 75 μM of MPT, respectively. The selected concentration of MPT was intentionally kept below the IC<sub>50(app)</sub> value of about 104 μM (determined with *N. europaea*; see Figure S3) to achieve an NO<sub>2</sub><sup>-</sup> production level that ranged from 25–44% of that observed in uninhibited cells. The Michaelis constant, *K<sub>m</sub>*, is the NH<sub>4</sub><sup>+</sup> concentration at which the reaction rate is 50% of the maximal rate, *V<sub>max</sub>* (see the Supporting Information).

The Michaelis–Menten plots show saturation kinetics, where the NO<sub>2</sub><sup>-</sup> production became independent of [NH<sub>4</sub><sup>+</sup>] beyond 0.5 mmol L<sup>-1</sup>. Furthermore, treatment with MPT did not lead to an increased NO<sub>2</sub><sup>-</sup> production even when [NH<sub>4</sub><sup>+</sup>] was increased by up to 4 orders of magnitude. Determination of the Michaelis–Menten parameters via hyperbolic analysis (data are included in Figure 3) revealed that *K<sub>m(app)</sub>* was unchanged within experimental error (*p* > 0.05), whereas *V<sub>max(app)</sub>* decreased with increasing [MPT]. Such a behavior is

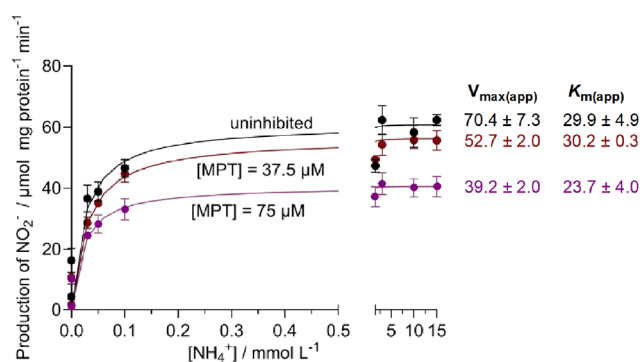


**Figure 3.** Effect of MPT on the  $\text{NO}_2^-$  production rate by *N. europaea* in dependence of  $[\text{NH}_4^+]$  after 60 min and Michaelis–Menten kinetic parameters  $V_{\max(\text{app})}$  in  $\mu\text{mol} (\text{mg protein min})^{-1}$  and  $K_{\text{m}(\text{app})}$  in  $\mu\text{M}$  (the suffix ‘app’ indicates that these constants were determined from bacterial cells and not the purified enzyme). The incubations were performed with  $[\text{NH}_4^+] = 0.003, 0.03, 0.05, 0.1, 1.5, 3.0, 10,$  and  $15 \text{ mM}$  in NaPB (pH = 7.5) with 1% (v/v) DMSO at  $30^\circ\text{C}$  and 100 rpm in the dark. Note the different axis scales to include the data at higher  $[\text{NH}_4^+]$ . Standard errors are errors of the mean calculated from three biological replicates (details in Table S6).

indicative for a noncompetitive inhibition mode,<sup>59</sup> i.e., MPT is not competing with  $\text{NH}_3$  for the same binding site in AMO. This inhibition mechanism is similar to that of phenylacetylene, whereas acetylene acts as a competitive inhibitor, which becomes less effective with increasing  $[\text{NH}_3]$ .<sup>46</sup> MPT’s mode of inhibition is also distinct from that of DMP and DCD, which are both uncompetitive inhibitors who bind to the AMO- $\text{NH}_3$  complex.<sup>30</sup>

**Determination of Toxic Effects of MPT.** To explore the potential toxic effects of MPT, a bacterial viability stain with cells of *N. europaea* was performed. The cells were incubated at  $30^\circ\text{C}$  with  $[\text{NH}_4^+] = 3 \text{ mM}$  for 12 h with  $[\text{MPT}] = 1.5 \text{ mM}$  (50 mol % of  $[\text{NH}_4^+]$ ). The control experiment in the absence of inhibitor was performed with  $[\text{NH}_4^+] = 3 \text{ mM}$  to avoid cell death caused by starvation. Analysis of ten microscopic images (the data for the individual images are shown in Table S7) revealed that the percentage of living cells upon treatment with MPT was  $75 \pm 8$  and that of dead cells was  $25 \pm 8$ . These data are within error similar to those obtained for the control

experiment (live =  $(83 \pm 10)\%$ ; dead =  $(17 \pm 10)\%$ ), indicating no acute toxicity of MPT for *N. europaea* at this concentration. Furthermore, ecotoxicity testing using a suite of freshwater and terrestrial indicator species did not reveal any acute (*Ceriodaphnia dubia*, *Melanotaenia splendida splendida*, *Eisenia fetida* and *Lactuca sativa*) or chronic (*Raphidocelis subcapitata*) toxicity of MPT (data are provided in Table S8).

**Measurement of  $\text{NH}_4^+$  and  $\text{NO}_3^-$  Profiles in Soil A.** To determine the nitrification inhibitory effect of MPT *in vivo*, soil incubations were performed by measuring concentration–time profiles for  $\text{NH}_4^+$  and  $\text{NO}_3^-$  in an acidic Australian soil (soil A, pH = 5.9 ( $\text{CaCl}_2$ )) over 21 days (Figure 4). MPT was tested at three different concentrations (0.5 mol %, 2.5 mol % and 5 mol % of applied fertilizer-N) and compared with the commercial inhibitor DMP (5 mol % of applied fertilizer-N). The  $\text{NH}_4^+$  and  $\text{NO}_3^-$  concentrations for all replicate runs, including errors and statistics, are compiled in Table S11.

Loss of  $\text{NH}_4^+$  occurred rapidly both without NI and with DMP, with negligible levels of  $\text{NH}_4^+$  remaining after 21 days of incubation (Figure 4a) and quantitative conversion to  $\text{NO}_3^-$  (Figure 4b). This result is consistent with the reported poor inhibitory performance of DMP in acidic soils.<sup>39,40,60</sup> Also, while MPT at the lowest application rate noticeably delayed  $\text{NH}_4^+$  loss within the first 15 days, it was not sufficiently effective to retain  $\text{NH}_4^+$  in the soil beyond 21 days.

In contrast, at the higher application rates of 2.5 and 5 mol %, MPT enabled to quantitatively suppress  $\text{NH}_4^+$  conversion in the soil with a statistical significance of  $p < 0.001$  over the entire incubation period when comparing inhibitor treatments to the control treatment with  $(\text{NH}_4)_2\text{SO}_4$  alone and when comparing to the 5 mol % DMP treatment. These findings were also reflected by the lack of  $\text{NO}_3^-$  production over the duration of the incubation. In fact, the inhibitory performance of MPT at the 2.5 mol % application rate was only marginally poorer than with the higher application rate of 5 mol % ( $p < 0.01$  for day 7 with 2.5 mol % MPT and  $p < 0.001$  for 2.5 and 5 mol % MPT on the other days). These data clearly illustrate MPT’s superior inhibitory performance, particularly compared to the current ‘gold standard’ DMP, which is likely a result of MPT’s distinct mode of inhibition.

**Measurement of  $\text{N}_2\text{O}$  Formation in Soils B – E.** As  $\text{N}_2\text{O}$  emissions from soils are controlled by biological

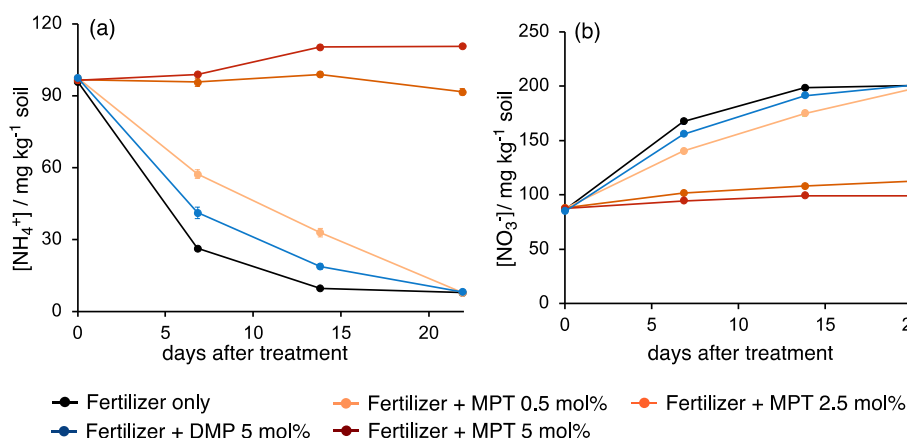


**Figure 4.** Mineral N-transformations in soil A (pH = 5.9 ( $\text{CaCl}_2$ )). Change in  $\text{NH}_4^+$  (a) and  $\text{NO}_3^-$  (b) concentrations over an incubation period of 21 days at  $25^\circ\text{C}$ . Detailed soil specifications are listed in Table S9.  $(\text{NH}_4)_2\text{SO}_4$  was used at an application rate of  $100 \text{ mg of N kg}^{-1}$  soil. Inhibitor treatments were 0.5 mol %, 2.5 mol % and 5 mol % of applied fertilizer-N for MPT, and 5 mol % for DMP, respectively. Each concentration profile was obtained from three replicates (for most data points the error bars are too small to be discernible).

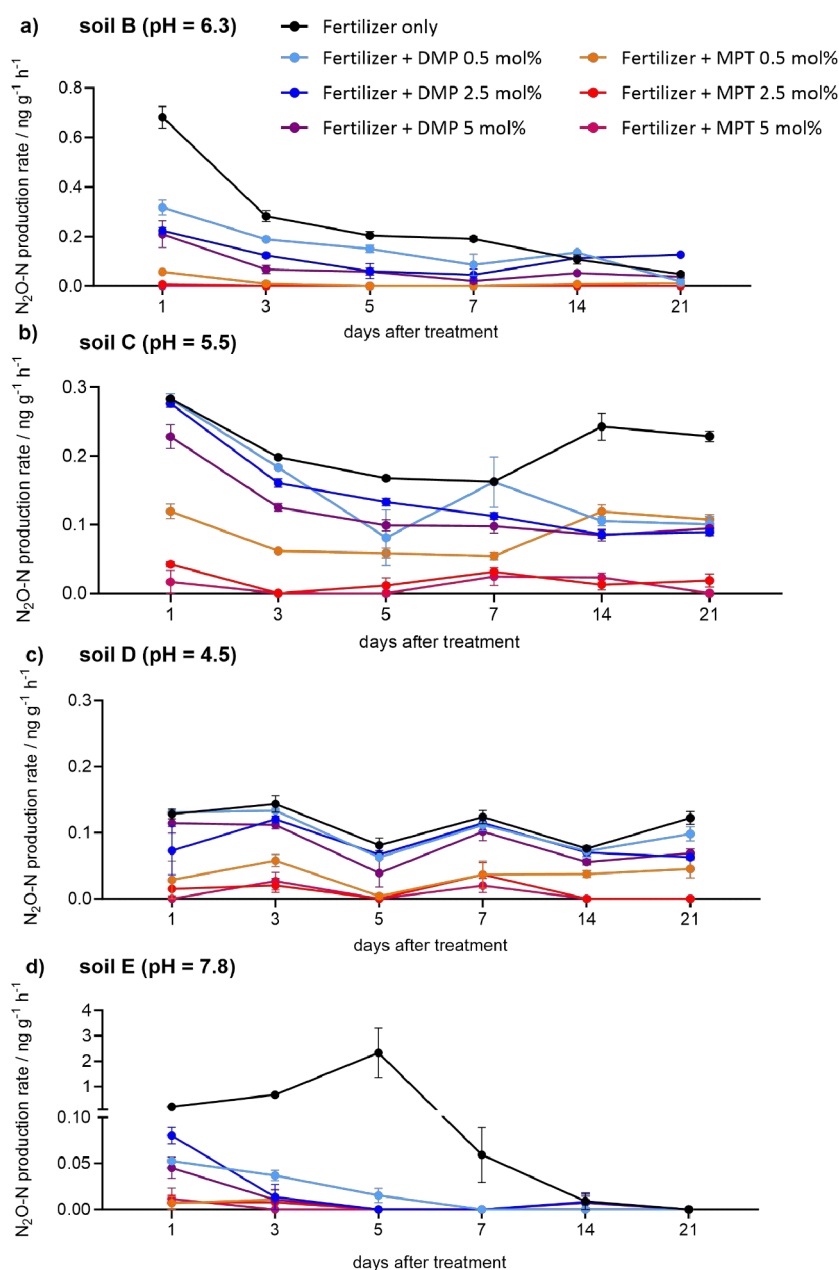


**Figure 5.**  $\text{N}_2\text{O-N}$  production rates over 21 days in soils B – E.  $(\text{NH}_4)_2\text{SO}_4$  was applied as 50 mg  $\text{kg}^{-1}$  soil ‘fertilizer only.’ [DMP] and [MPT] were 0.5 mol %, 2.5 mol % and 5 mol % of the applied fertilizer-N, respectively. Data were calculated from three biological replicates. Detailed soil specifications are listed in Table S9. Soil E: note the different axis scale to include higher  $\text{N}_2\text{O}$  production rates; no  $\text{N}_2\text{O}$  production was detected beyond day 5 for DMP at 5 mol % and all MPT treatments (for many data points the error bars are too small to be discernible).

nitrification-denitrification pathways, retention of  $\text{NH}_4^+$  in the soil through the use of MPT should also reduce formation of  $\text{N}_2\text{O}$ .<sup>10,61</sup> To validate this, incubations were performed with four different German soils (soils B – E) with varying pH, and the  $\text{N}_2\text{O}$  production rates in the presence of MPT were compared with those measured using DMP at the same application rates (i.e., 0.5 mol %, 2.5 mol % and 5 mol % of applied fertilizer-N; details are provided in Table S10) as well as in the absence of NI (Figure 5). The individual data, including errors and statistics, are listed in Table S12.

In the first week after fertilizer application to soil B (pH = 6.3 ( $\text{CaCl}_2$ )), the  $\text{N}_2\text{O-N}$  production rate in the uninhibited soil was the highest with 0.68  $\text{ng g}^{-1}$  soil  $\text{h}^{-1}$  at day 1 and 0.19  $\text{ng g}^{-1}$  soil  $\text{h}^{-1}$  at day 7, reflecting the initial high N availability,

before gradually dropping to 0.05  $\text{ng g}^{-1}$  soil  $\text{h}^{-1}$  at day 21 (Figure 5a). Treatment with DMP slowed down  $\text{N}_2\text{O}$  formation in dependence on the application rate. With 0.5 mol % of DMP the  $\text{N}_2\text{O}$  production rate at day 1 was with 0.32  $\text{ng g}^{-1}$  soil  $\text{h}^{-1}$  approximately 50% of that in the uninhibited soil. At the higher application rates of 2.5 mol % and 5 mol % DMP, the  $\text{N}_2\text{O}$  production rate dropped by approximately 67% of that in the absence of the inhibitor. On the other hand, soil treated with MPT produced  $\text{N}_2\text{O}$  at a rate of only 0.06  $\text{ng g}^{-1}$  soil  $\text{h}^{-1}$  at day 1 in the case of the lowest application rate, otherwise the amount of  $\text{N}_2\text{O}$  remained below the detection limit over the duration of the experiment, clearly demonstrating that MPT is much more effective in reducing  $\text{N}_2\text{O}$  formation than DMP.

In the soil with higher acidity, soil C (pH = 5.5 (CaCl<sub>2</sub>)), a decrease in the N<sub>2</sub>O production rate was observed in the uninhibited soil compared to soil B (see Figure 5b). This reduction is likely linked to the diminished amount of NH<sub>3</sub> available for oxidation by AMO due to protonation to NH<sub>4</sub><sup>+</sup>. The average rate of N<sub>2</sub>O production remained largely unchanged over the entire 21 days, confirming that in acidic soils NH<sub>3</sub> can be effectively retained as NH<sub>4</sub><sup>+</sup>.<sup>62</sup> Soil treated with 0.5 and 2.5 mol % of DMP did not show a significantly reduced N<sub>2</sub>O formation rate in the first 2 weeks ( $p > 0.05$ ) compared to the uninhibited soil. Only at the highest application rate of DMP, a gradual reduction of the N<sub>2</sub>O production rate to 0.095 ng g<sup>-1</sup> soil h<sup>-1</sup> at day 21 was found. In comparison, soil treated with 0.5 mol % of MPT produced about 0.12 ng g<sup>-1</sup> soil h<sup>-1</sup> of N<sub>2</sub>O over the duration of the incubation, which is just 25% of the amount released from the uninhibited soil. At the higher MPT application rates, the production of N<sub>2</sub>O was nearly completely suppressed.

The most acidic soil (soil D, pH = 4.7 (CaCl<sub>2</sub>)) produced the lowest amount of N<sub>2</sub>O, ranging from 0.08 to 0.14 ng g<sup>-1</sup> soil h<sup>-1</sup> throughout the experiment (Figure 5c). No significant difference of the N<sub>2</sub>O production rates between the uninhibited soil and soil treated with DMP was found at any time point ( $p > 0.05$ ). These data align with the NH<sub>4</sub><sup>+</sup>/NO<sub>3</sub><sup>-</sup> profiles measured in this work (see Figure 3) and literature.<sup>26,38</sup> In contrast, soil treated with MPT at 0.5 mol % slowed down N<sub>2</sub>O production by 60%, whereas MPT at the two higher application rates reduced the N<sub>2</sub>O production rate to practically zero from the start of the experiment, indicating that the inhibitory performance of MPT is essentially pH-independent at these concentrations.

Soil E (pH = 7.5 (CaCl<sub>2</sub>)) was collected from an agricultural recultivation site of a former open-cast brown coal mine. Recultivation soils are usually low in nutrients, such as N.<sup>63–66</sup> This lack of N retention capacity resulted in an unusual N<sub>2</sub>O profile in the uninhibited soil, where the N<sub>2</sub>O production rate rapidly increased within the first 5 days following fertilizer application, reaching a maximum of 2.33 ng g<sup>-1</sup> soil h<sup>-1</sup> at day 5, before declining again to practically zero at day 14, indicating a depleted N availability (Figure 5d). This behavior indicates a very high nitrification/denitrification activity of this soil, which quickly adapts to N fertilization. Treatment with DMP and MPT led to a dampening of the N<sub>2</sub>O production, with MPT being considerably more effective than DMP in the first 5 days. Beyond that time point, the rate of N<sub>2</sub>O production in the presence of either inhibitor remained extremely low.

**qPCR Measurements in Soils B – E.** To assess the effect of the irreversibly acting inhibitor MPT on the nitrifier community, a quantitative analysis of the DNA *amoA* bacterial and archaeal gene copies was carried out in soils B – E at day 22 of the incubation for untreated soils (H<sub>2</sub>O added only), fertilizer-only treated soils ((NH<sub>4</sub>)<sub>2</sub>SO<sub>4</sub>), and both MPT and DMP (as benchmark) treated soils at an application rate of 5 mol % of applied fertilizer-N. Figure 6 shows that nitrifying archaea were the more abundant microorganisms in these four soils. Thus, the *amoA* gene copies for AOA were in the range of 1.2–35 × 10<sup>7</sup> gene copies g<sup>-1</sup> wet soil, whereas those for AOB ranged from 3.3–56 × 10<sup>5</sup> gene copies g<sup>-1</sup> wet soil (detailed data including errors and statistics, are given in Table S13).

No significant change in the bacterial *amoA* population was found in the untreated versus fertilized soils B – D ( $p > 0.05$ ),

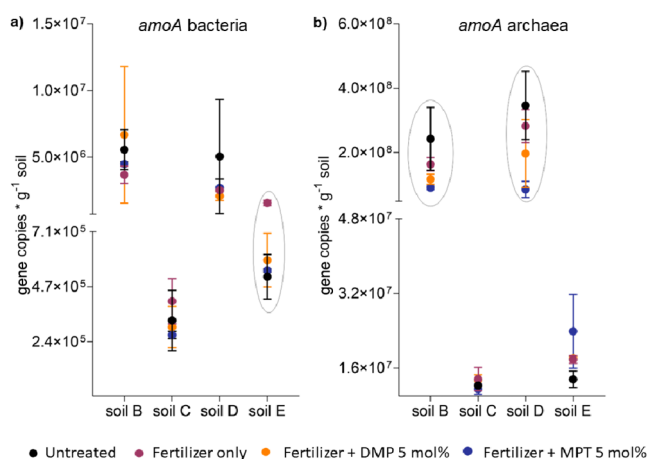


**Figure 6.** qPCR analysis of soils B – E. Bacterial (a) and archaeal (b) *amoA* gene copy numbers per g of soil determined at day 22 of incubation in soils B (pH = 6.3), C (pH = 5.5), D (pH = 4.7), and E (pH = 7.5). ‘Untreated’ soil contained only deionized water as additive, ‘fertilizer only’ contained (NH<sub>4</sub>)<sub>2</sub>SO<sub>4</sub> at an application rate of 50 mg N kg<sup>-1</sup> soil, likewise as the NI treated soils. The inhibitors MPT and DMP were applied at 5 mol % of applied fertilizer-N. Note the different axis scales to include the data with higher copy numbers. Each data point was calculated from three biological replicates. Circled data sets indicate significant differences of *amoA* gene abundances ( $p < 0.05$ ) between different treatments (see text).

respectively (Figure 6a). Interestingly, in soil E the *amoA* gene copies for AOB increased 3-fold from 5.1 × 10<sup>5</sup> to 1.6 × 10<sup>6</sup> gene copies g<sup>-1</sup> soil upon fertilizer treatment. This bacterial growth correlated with the enhanced N<sub>2</sub>O production at the beginning of the experiment (see Figure 5d). Treatment of soils B – D with fertilizer and either MPT or DMP did not lead to a significant change in the bacterial *amoA* population compared to the untreated or fertilized soils, respectively ( $p > 0.05$ ). In the case of soil E treated with fertilizer and DMP or MPT, respectively, the population dropped to the value of the unfertilized soil ( $p < 0.05$ ), suggesting that both NIs have an effect on the activity and therewith prevent growth of AOB. Overall, the impact of DMP and MPT on the AOB community appears to be similar.

In the case of the archaeal population, a similar response to fertilization across all soils was found, as no increase of gene copies in fertilized compared to untreated soils was detected (Figure 6b). On the other hand, a significant reduction of *amoA* gene copies was found in soils B and D after treatment with MPT compared to the respective untreated soils ( $p = 0.02$ ). Thus, in soil B the average gene abundance dropped by 40% from 2.4 × 10<sup>8</sup> gene copies g<sup>-1</sup> soil for the untreated soil to 9.0 × 10<sup>7</sup> gene copies g<sup>-1</sup> soil for the MPT treated soil. In soil D the population dropped by 24% from an average of 3.5 × 10<sup>8</sup> gene copies g<sup>-1</sup> soil to 8.5 × 10<sup>7</sup> gene copies g<sup>-1</sup> soil. In contrast, no decrease of archaeal *amoA* gene copies by DMP was found in any of the soils, confirming the reported low efficacy of this inhibitor against archaeal strains.<sup>38,60,67–70</sup> Interestingly, MPT had an effect on the *amoA* gene copies only in particular soils and not throughout all soil types. On the other hand, from the finding that none of the three DMP treatments reduced the N<sub>2</sub>O emission in the most acidic soil D to a considerable extent, whereas MPT inhibited nitrification up to 100% for 21 days (Figure 5c), these data indicate an enhanced inhibitory effect of MPT on archaeal strains. It can therefore be concluded that the performance of MPT is not

only independent of soil pH but also independent of the AMO orthologue. Overall, our study with MPT provides support for our hypothesis that NIs need to operate through an irreversible mechanism in order to achieve a consistent excellent performance across different agroecosystems, which is urgently required to increase NUE in agriculture.

The distinctive benefit of MPT lies in its ease of synthesis in the laboratory, achieving high yields through a one-pot reaction using readily available starting materials.<sup>50</sup> This characteristic opens up exciting prospects for commercialization. In the upcoming stage of our inhibitor development, we intend to scrutinize the technical and economic feasibility of producing an MPT on a commercial scale. Additional work involves the development of formulating protocols, evaluating the longevity of the active ingredient in both the formulation and the fertilizer, and conducting assessments of phytotoxicity through glasshouse studies, along with agronomy evaluations in field campaigns.

## ■ ASSOCIATED CONTENT

### SI Supporting Information

The Supporting Information is available free of charge at <https://pubs.acs.org/doi/10.1021/acsagscitech.3c00506>.

Synthetic protocols for MPT and H-MPT, including spectroscopic data. Protocols of the bacterial studies, toxicity tests, qPCR studies and soil incubations (mineral-N transformations and N<sub>2</sub>O measurements). Supplementary Table S1 (NH<sub>4</sub><sup>+</sup>-dependent NO<sub>2</sub><sup>-</sup> production after treating *N. europaea* and *N. multiformis* with MPT and H-MPT); Table S2 (NH<sub>4</sub><sup>+</sup>-dependent NO<sub>2</sub><sup>-</sup> production after treating *N. europaea* and *N. multiformis* with NI-1, NI-2 and NI-3); Table S3 (NH<sub>2</sub>OH-dependent NO<sub>2</sub><sup>-</sup> production after treating *N. europaea* and *N. multiformis* with MPT); Table S4 (rate coefficients for the time-dependent O<sub>2</sub> consumption by *N. europaea* in the absence of MPT); Table S5 (rate coefficients for the inhibition of *N. europaea* by MPT at different concentrations, as determined by O<sub>2</sub> consumption); Table S6 (Michaelis–Menten kinetic parameters of the [NH<sub>4</sub><sup>+</sup>]-dependent production of NO<sub>2</sub><sup>-</sup> by *N. europaea* determined via hyperbolic analysis in the absence and presence of MPT at two different MPT concentrations); Table S7 (number of alive and dead cells of *N. europaea* in the absence and presence of MPT determined with a bacterial viability stain); Table S8 (half-maximal effective concentrations for MPT and DMP determined by toxicity testing to a suite of freshwater and terrestrial ecotoxicity tests); Table S9 (specifications of the soils studied in this work); Table S10 (application rates of DMP and MPT and weight % of total (NH<sub>4</sub>)<sub>2</sub>SO<sub>4</sub> applied to soils B–E); Table S11 (soil incubation studies to determine mineral-N conversion in soil A); Table S12 (N<sub>2</sub>O production rates for soils B–E); Table S13 (calculated gene abundances of *amoA* from bacteria and archaea after 22 days of incubation). Supplementary Figure S1 (O<sub>2</sub> consumption by *N. europaea* as a function of time before the addition of MPT); Figure S2 (first order decay exponential fit of O<sub>2</sub> consumption by *N. europaea* as a function of time after the addition of MPT); Figure S3 (determination of the IC<sub>50(app)</sub> value for MPT) (PDF)

## ■ AUTHOR INFORMATION

### Corresponding Author

Uta Wille – School of Chemistry, The University of Melbourne, Parkville, Victoria 3010, Australia; [orcid.org/0000-0003-1756-5449](https://orcid.org/0000-0003-1756-5449); Phone: +61 3 8344 2425; Email: [uwille@unimelb.edu.au](mailto:uwille@unimelb.edu.au)

### Authors

Sibel C. Yildirim – School of Chemistry, The University of Melbourne, Parkville, Victoria 3010, Australia; Institute of Crop Science and Resource Conservation, University of Bonn, Bonn 53115, Germany; Institute of Bio- and Geosciences, Agrosphere (IBG-3), Forschungszentrum Jülich GmbH, Jülich 52428, Germany

Josef G. Nathanael – School of Chemistry, The University of Melbourne, Parkville, Victoria 3010, Australia

Katharina Frindt – Institute of Crop Science and Resource Conservation, University of Bonn, Bonn 53115, Germany

Otávio dos Anjos Leal – Institute of Bio- and Geosciences, Agrosphere (IBG-3), Forschungszentrum Jülich GmbH, Jülich 52428, Germany; [orcid.org/0000-0003-2786-4119](https://orcid.org/0000-0003-2786-4119)

Robert M. Walker – School of BioSciences, The University of Melbourne, Parkville, Victoria 3010, Australia

Ute Roessner – School of BioSciences, The University of Melbourne, Parkville, Victoria 3010, Australia; Research School of Biology, The Australian National University, Acton, Australian Capital Territory 2600, Australia; [orcid.org/0000-0002-6482-2615](https://orcid.org/0000-0002-6482-2615)

Claudia Knief – Institute of Crop Science and Resource Conservation, University of Bonn, Bonn 53115, Germany

Nicolas Brüggemann – Institute of Bio- and Geosciences, Agrosphere (IBG-3), Forschungszentrum Jülich GmbH, Jülich 52428, Germany

Complete contact information is available at:

<https://pubs.acs.org/10.1021/acsagscitech.3c00506>

### Author Contributions

S. C. Y performed all experiments (mineral-N retention experiment performed by J. G. N.), processed the experimental data and performed the analysis. R. W., U. R., N. B., K. F., O. A. L., C. K. and U. W. designed, planned and supervised the work. All authors aided in interpreting the results. S. C. Y. and U. W. wrote the manuscript and designed the figures with input of all authors. All authors reviewed, edited and approved the manuscript.

### Funding

This work was supported by the Australian Research Council through the ‘ARC Research Hub for Smart Fertilisers’ (IH200100023) and Discovery Project (‘Connecting soil nitrogen and plant uptake for greener agriculture,’ DP200101162) Schemes.

### Notes

The authors declare no competing financial interest.

## ■ ACKNOWLEDGMENTS

We thank Guy Jamesson, Paul Donnelly, Franz Leistner, Bethany Taggart, Parvinder Sidhu, Helen Suter and Deli Chen for their support and Rick Krasso for the exotoxicological studies. Support by the Jülich-University of Melbourne Postgraduate Academy (JUMPA), the Bio21 Institute’s



Magnetic Resonance and the Mass Spectrometry and Proteomics Facility (MSPF) are gratefully acknowledged.

## ABBREVIATIONS

AMO	ammonia monooxygenase
AOB	ammonia oxidizing bacteria
BCA	bicinchoninic acid assay
DCD	dicyandiamide
DMP	3,4-dimethyl-1H-pyrazole
DMPG	3,4-dimethyl-1H-pyrazole glycolate
DMPP	3,4-dimethyl-1H-pyrazole phosphate
DMSO	dimethyl sulfoxide
H-MPT	4-methyl-1-propyl-1H-1,2,3-triazole
IC <sub>50</sub>	concentration of inhibitor to decrease response to 50%
K <sub>m</sub>	Michaelis–Menten constant
MPT	4-methyl-1-(prop-2-yn-1-yl)-1H-1,2,3-triazole
NaPB	sodium phosphate buffer
NI	nitrification inhibitor
<i>N. europaea</i>	<i>Nitrosomonas europaea</i>
<i>N. multiformis</i>	<i>Nitrospira multiformis</i>
NUE	nitrogen use efficiency
PM <sub>2.5</sub>	fine particulate matter (particles less than 2.5 μm in diameter)
qPCR	quantitative polymerase chain reaction
rpm	rotations per minute
SAR	structure activity relationship
V <sub>max</sub>	maximal rate of enzymatic reaction

## REFERENCES

- Godfray, H. C. J.; Beddington, J. R.; Crute, I. R.; Haddad, L.; Lawrence, D.; Muir, J. F.; Pretty, J.; Robinson, S.; Thomas, S. M.; Toulmin, C. Food Security: The Challenge of Feeding 9 Billion People. *Science* **2010**, *327*, 812–818.
- Lin, B.-L.; Sakoda, A.; Shibasaki, R.; Suzuki, M. A Modelling Approach to Global Nitrate Leaching Caused by Anthropogenic Fertilisation. *Water Res.* **2001**, *35* (8), 1961–1968.
- Raun, W. R.; Schepers, J. S. Nitrogen Management for Improved Use Efficiency. In *Nitrogen in Agricultural Systems*, Schepers, J. S. R.; Raun, W. R., Eds.; Wiley, 2008; pp. 675–693.
- Cavigelli, M. A.; Del Grosso, S. J.; Liebig, M. A.; Snyder, C. S.; Fixen, P. E.; Venterea, R. T.; Leytem, A. B.; McLain, J. E.; Watts, D. B. US Agricultural Nitrous Oxide Emissions: Context, Status, and Trends. *Front. Ecol. Environ.* **2012**, *10*, 537–546.
- Ladha, J. K.; Pathak, H. J.; Krupnik, T.; Six, J.; van Kessel, C. Efficiency of Fertilizer Nitrogen in Cereal Production: Retrospects and Prospects. In *Advances in Agronomy*, Academic Press, 2005; Vol. 87, pp. 85–156.
- Robertson, G. P.; Bruulsema, T. W.; Gehl, R. J.; Kanter, D.; Mauzerall, D. L.; Rotz, C. A.; Williams, C. O. Nitrogen–Climate Interactions in US Agriculture. *Biogeochemistry* **2013**, *114*, 41–70.
- Norton, J.; Ouyang, Y. Controls and Adaptive Management of Nitrification in Agricultural Soils. *Front. Microbiol.* **2019**, *10*, 1931.
- Jetten, M. S. M. The Microbial Nitrogen Cycle. *Environ. Microbiol.* **2008**, *10*, 2903–2909.
- Coskun, D.; Britto, D. T.; Shi, W.; Kronzucker, H. J. Nitrogen Transformations in Modern Agriculture and the Role of Biological Nitrification Inhibition. *Nature Plants* **2017**, *3*, 17074.
- Ruser, R.; Schulz, R. The Effect of Nitrification Inhibitors on the Nitrous Oxide (N<sub>2</sub>O) Release from Agricultural Soils—a Review. *J. Plant Nutr. Soil Sci.* **2015**, *178*, 171–188.
- Lawton, T. J.; Ham, J.; Sun, T.; Rosenzweig, A. C. Structural Conservation of the B Subunit in the Ammonia Monooxygenase/Particulate Methane Monooxygenase Superfamily. *Proteins* **2014**, *82*, 2263–2267.
- McTavish, H.; Fuchs, J. A.; Hooper, A. B. Sequence of the Gene Coding for Ammonia Monooxygenase in *Nitrosomonas europaea*. *J. Bacteriol.* **1993**, *175*, 2436.
- Musiani, F.; Broll, V.; Evangelisti, E.; Ciurli, S. The Model Structure of the Copper-Dependent Ammonia Monooxygenase. *J. Biol. Inorg. Chem.* **2020**, *25*, 995–1007.
- McCarty, G. W. Modes of Action of Nitrification Inhibitors. *Biol. Fertil. Soils* **1999**, *29*, 1–9.
- Hyman, M. R.; Sansome-Smith, A. W.; Shears, J. H.; Wood, P. M. A Kinetic Study of Benzene Oxidation to Phenol By Whole Cells of *Nitrosomonas europaea* and Evidence for the Further Oxidation of Phenol to Hydroquinone. *Arch. Microbiol.* **1985**, *143*, 302–306.
- Caranto, J. D.; Lancaster, K. M. Nitric Oxide is an Obligate Bacterial Nitrification Intermediate Produced by Hydroxylamine Oxidoreductase. *Proc. Natl. Acad. Sci. U. S. A* **2017**, *114*, 8217–8222.
- Caranto, J. D.; Vilbert, A. C.; Lancaster, K. M. *Nitrosomonas europaea* Cytochrome P460 is a Direct Link Between Nitrification and Nitrous Oxide Emission. *Proc. Natl. Acad. Sci. U. S. A* **2016**, *113*, 14704–14709.
- Venterea, R. T.; Rolston, D. E. Mechanisms and Kinetics of Nitric and Nitrous Oxide Production During Nitrification in Agricultural Soil. *Global Change Biol.* **2000**, *6*, 303–316.
- Wrage-Mönnig, N.; Horn, M. A.; Well, R.; Müller, C.; Velthof, G.; Oenema, O. The Role of Nitrifier Denitrification in the Production of Nitrous Oxide Revisited. *Soil Biol. Biochem.* **2018**, *123*, A3–A16.
- Sun, D.; Tang, X.; Zhao, M.; Zhang, Z.; Hou, L.; Liu, M.; Wang, B.; Klümper, U.; Han, P. Distribution and Diversity of Comammox Nitrospira in Coastal Wetlands of China. *Front. Microbiol.* **2020**, *11*, 589268.
- Zerulla, W.; Barth, T.; Dressel, J.; Erhardt, K.; Pasda, G.; Rädle, M.; Wissemeyer, A. 3,4-Dimethylpyrazole Phosphate (DMPP) – A new Nitrification Inhibitor for Agriculture and Horticulture. *Biol. Fertil. Soils* **2001**, *34*, 79–84.
- Pasda, G.; Hähndel, R.; Zerulla, W. Effect of Fertilizers With the new Nitrification Inhibitor DMPP (3,4-Dimethylpyrazole phosphate) on Yield and Quality of Agricultural and Horticultural Crops. *Biol. Fertil. Soils* **2001**, *34*, 85–97.
- Barrena, I.; Menéndez, S.; Correa-Galeote, D.; Vega-Mas, I.; Bedmar, E. J.; González-Murua, C.; Estavillo, J. M. Soil Water Content Modulates the Effect of the Nitrification Inhibitor 3,4-Dimethylpyrazole phosphate (DMPP) on Nitrifying and Denitrifying Bacteria. *Geoderma* **2017**, *303*, 1–8.
- Li, H.; Liang, X.; Chen, Y.; Lian, Y.; Tian, G.; Ni, W. Effect of Nitrification Inhibitor DMPP on Nitrogen Leaching, Nitrifying Organisms, and Enzyme Activities in a Rice–Oilseed Rape Cropping System. *J. Environ. Sci.* **2008**, *20*, 149–155.
- Menéndez, S.; Merino, P.; Pinto, M.; González-Murua, C.; Estavillo, J. M. 3,4-Dimethylpyrazol Phosphate Effect on Nitrous Oxide, Nitric Oxide, Ammonia, and Carbon Dioxide Emissions from Grasslands. *J. Environ. Qual.* **2006**, *35*, 973–981.
- Dougherty, W. J.; Collins, D.; Van Zwieten, L.; Rowlings, D. W. Nitrification (DMPP) and Urease (NBPT) Inhibitors had no Effect on Pasture Yield, Nitrous Oxide Emissions, or Nitrate Leaching under Irrigation in a Hot-Dry Climate. *Soil Res.* **2016**, *54*, 675–683.
- Menéndez, S.; Barrena, I.; Setien, I.; González-Murua, C.; Estavillo, J. M. Efficiency of Nitrification Inhibitor DMPP to Reduce Nitrous Oxide Emissions Under Different Temperature and Moisture Conditions. *Soil Biol. Biochem.* **2012**, *53*, 82–89.
- Nauer, P. A.; Fest, B. J.; Visser, L.; Arndt, S. K. On-Farm Trial on the Effectiveness of the Nitrification Inhibitor DMPP Indicates no Benefits Under Commercial Australian Farming Practices. *Agric. Ecosyst. Environ.* **2018**, *253*, 82–89.
- Suter, H.; Lam, S. K.; Walker, C.; Chen, D. Benefits from Enhanced-Efficiency Nitrogen Fertilisers in Rainfed Temperate Pastures are Seasonally Driven. *Soil Res.* **2022**, *60*, 147–157.
- Yildirim, S. C.; Walker, R. M.; Roessner, U.; Wille, U. Assessing the Efficacy, Acute Toxicity, and Binding Modes of the Agricultural Nitrification Inhibitors 3,4-Dimethyl-1H-pyrazole (DMP) and

- Dicyandiamide (DCD) With *Nitrosomonas europaea*. *ACS Agric. Sci. Technol.* **2023**, *3*, 222–231.
- (31) Venterea, R. T.; Clough, T. J.; Coulter, J. A.; Souza, E. F. C.; Breuillin-Sessoms, F.; Spokas, K. A.; Sadowsky, M. J.; Gupta, S. K.; Bronson, K. F. Temperature Alters Dicyandiamide (DCD) Efficacy for Multiple Reactive Nitrogen Species in Urea-Amended Soils: Experiments and Modeling. *Soil Biol. Biochem.* **2021**, *160*, 108341.
- (32) Ray, A.; Forrestal, P.; Nkwonta, C.; Rahman, N.; Byrne, P.; Danaher, M.; Richards, K.; Hogan, S.; Cummins, E. Modelling Potential Human Exposure to the Nitrification Inhibitor Dicyandiamide Through the Environment-Food Pathway. *Environ. Impact Assess. Rev.* **2023**, *101*, 107082.
- (33) Nanayakkara, D.; Prashantha, M. A. B.; Fernando, T. L. D.; Dissanayake, C. K.; Karunarathna, B. Detection and Quantification of Dicyandiamide (DCD) Adulteration in Milk Using Infrared Spectroscopy: A Rapid and Cost-Effective Screening Approach. *Food And Humanity* **2023**, *1*, 1472–1481.
- (34) Casali, L.; Broll, V.; Ciurli, S.; Emmerling, F.; Braga, D.; Grepioni, F. Facilitating Nitrification Inhibition Through Green, Mechanochemical Synthesis of a Novel Nitrapyrin Complex. *Cryst. Growth Des.* **2021**, *21*, 5792–5799.
- (35) Zaller, J. G.; Kruse-Plaß, M.; Schlechtriemen, U.; Gruber, E.; Peer, M.; Nadeem, I.; Formayer, H.; Hutter, H.-P.; Landler, L. Unexpected Air Pollutants With Potential Human Health Hazards: Nitrification Inhibitors, Biocides, and Persistent Organic Substances. *Sci. Total Environ.* **2023**, *862*, 160643.
- (36) Guardia, G.; Marsden, K. A.; Vallejo, A.; Jones, D. L.; Chadwick, D. R. Determining the Influence of Environmental and Edaphic Factors on the Fate of the Nitrification Inhibitors DCD and DMPP in Soil. *Sci. Total Environ.* **2018**, *624*, 1202–1212.
- (37) Koci, J.; Nelson, P. N. Tropical Dairy Pasture Yield and Nitrogen Cycling: Effect of Urea Application Rate and a Nitrification Inhibitor, DMPP. *Crop Pasture Sci.* **2016**, *67*, 766–779.
- (38) Li, A.-R.; Song, X.-T.; Bakken, L. R.; Ju, X.-T. Reduction of N<sub>2</sub>O Emissions by DMPP Depends on the Interactions of Nitrogen Sources (Digestate vs. Urea) With Soil Properties. *J. Integr. Agric.* **2023**, *22*, 251–264.
- (39) Kaveney, B.; Condon, J.; Doran, G.; Galea, F.; Rigg, J. Soil Moisture Impacts Nitrification From Nitrogen Fertilisers Treated with 3,4-Dimethylpyrazole Phosphate in Acidic Soils. *Soil Res.* **2022**, *60*, 86–101.
- (40) Tufail, M. A.; Irfan, M.; Umar, W.; Wakeel, A.; Schmitz, R. A. Mediation of Gaseous Emissions and Improving Plant Productivity by DCD and DMPP Nitrification Inhibitors: Meta-Analysis of Last Three Decades. *Environ. Sci. Pollut. Res. Int.* **2023**, *30*, 64719–64735.
- (41) Ensign, S. A.; Hyman, M. R.; Arp, D. J. *In vitro* Activation of Ammonia Monooxygenase from *Nitrosomonas europaea* by Copper. *J. Bacteriol.* **1993**, *175*, 1971–1980.
- (42) Lieberman, R. L.; Rosenzweig, A. C. Crystal Structure of a Membrane-Bound Metalloenzyme That Catalyses the Biological Oxidation of Methane. *Nature* **2005**, *434*, 177–182.
- (43) Cao, L.; Caldararu, O.; Rosenzweig, A. C.; Ryde, U. Quantum Refinement Does not Support Dinuclear Copper Sites in Crystal Structures of Particulate Methane Monooxygenase. *Angew. Chem. Int. Ed.* **2018**, *57*, 162–166.
- (44) McCarty, G. W.; Bremner, J. M. Inhibition of Nitrification in Soil by Heterocyclic Nitrogen Compounds. *Biol. Fertil. Soils* **1989**, *8* (3), 204–211.
- (45) Hyman, M. R.; Wood, P. M. Suicidal inactivation and labelling of ammonia mono-oxygenase by acetylene. *Biochem. J.* **1985**, *227*, 719–725.
- (46) Wright, C. L.; Schatteman, A.; Crombie, A. T.; Murrell, J. C.; Lehtovirta-Morley, L. E.; Stams, A. J. M. Inhibition of Ammonia Monooxygenase from Ammonia-Oxidizing Archaea by Linear and Aromatic Alkynes. *Appl. Environ. Microbiol.* **2020**, *86*, No. e02388–02319.
- (47) Lontoh, S.; DiSpirito, A. A.; Krema, C. L.; Whittaker, M. R.; Hooper, A. B.; Semrau, J. D. Differential Inhibition *In Vivo* of Ammonia Monooxygenase, Soluble Methane Monooxygenase and Membrane-Associated Methane Monooxygenase by Phenylacetylene. *Environ. Microbiol.* **2000**, *2*, 485–494.
- (48) Taggert, B. I.; Walker, C.; Chen, D.; Wille, U. Substituted 1, 2, 3-Triazoles: A New Class of Nitrification Inhibitors. *Sci. Rep.* **2021**, *11*, 1–12.
- (49) Yildirim, S. C.; Walker, R. M.; Roessner, U.; Wille, U. Rapid and Inexpensive Assay for Testing the Efficiency of Potential new Synthetic Nitrification Inhibitors. *ACS Agric. Sci. Technol.* **2023**, *3*, 260–269.
- (50) Clark, P. R.; Williams, G. D.; Hayes, J. F.; Tomkinson, N. C. A Scalable Metal-, Azide-, and Halogen-Free Method for the Preparation of Triazoles. *Angew. Chem. Int. Ed.* **2020**, *59*, 6740–6744.
- (51) Yildirim, S. C.; Taggert, B. I.; Walker, R. M.; Roessner, U.; Wille, U. Insights into the Efficacy and Binding Mode of 1,4-Disubstituted 1,2,3-Triazoles—A New Class of Agricultural Nitrification Inhibitors. *ACS Agric. Sci. Technol.* **2023**, *3*, 260–269.
- (52) Li, Z.; Reichel, R.; Brüggemann, N. Effect of C: N: P Stoichiometry on Soil Nitrous Oxide Emission and Nitrogen Retention. *J. Soil Sci. Plant Nutr.* **2021**, *184*, 520–529.
- (53) Reichel, R.; Wei, J.; Islam, M. S.; Schmid, C.; Wissel, H.; Schröder, P.; Schloter, M.; Brüggemann, N. Potential of Wheat Straw, Spruce Sawdust, and Lignin as High Organic Carbon Soil Amendments to Improve Agricultural Nitrogen Retention Capacity: An Incubation Study. *Front. Plant Sci.* **2018**, *9*, 900.
- (54) Christopher, A. F.; Kathryn, J. R.; Beman, J. M.; Alyson, E. S.; Brian, B. O. Ubiquity and Diversity of Ammonia-Oxidizing Archaea in Water Columns and Sediments of the Ocean. *Proc. Natl. Acad. Sci. U. S. A.* **2005**, *102*, 14683–14688.
- (55) Rothhauwe, J. H.; Witzel, K. P.; Liesack, W. The Ammonia Monooxygenase Structural Gene *amoA* as a Functional Marker: Molecular Fine-Scale Analysis of Natural Ammonia-Oxidizing Populations. *Appl. Environ. Microbiol.* **1997**, *63*, 4704–4712.
- (56) Hyman, M. R.; Arp, D. J. <sup>14</sup>C<sub>2</sub>H<sub>2</sub>- and <sup>14</sup>CO<sub>2</sub>-Labeling Studies of the *De Novo* Synthesis of Polypeptides by *Nitrosomonas europaea* During Recovery from Acetylene and Light Inactivation of Ammonia Monooxygenase. *J. Biol. Chem.* **1992**, *267*, 1534–1545.
- (57) Arp, D. J.; Sayavedra-Soto, L. A.; Hommes, N. G. Molecular Biology and Biochemistry of Ammonia Oxidation by *Nitrosomonas europaea*. *Arch. Microbiol.* **2002**, *178*, 250–255.
- (58) Schatteman, A.; Wright, C. L.; Crombie, A. T.; Murrell, J. C.; Lehtovirta-Morley, L. E. Hydrazines as Substrates and Inhibitors of the Archaeal Ammonia Oxidation Pathway. *Appl. Environ. Microbiol.* **2022**, *88*, No. e02470–02421.
- (59) Delaune, K. P.; Alsayouri, K. Physiology, Noncompetitive Inhibitor. In *StatPearls Publishing [internet]*, StatPearls Publishing, 2022.
- (60) Shi, X.; Hu, H.; He, J.; Chen, D.; Suter, H. C. Effects of 3,4-Dimethylpyrazole Phosphate (DMPP) on Nitrification and the Abundance and Community Composition of Soil Ammonia Oxidizers in Three Land Uses. *Biol. Fertil. Soils* **2016**, *52*, 927–939.
- (61) Guzman-Bustamante, I.; Schulz, R.; Müller, T.; Ruser, R. Split N Application and DMP Based Nitrification Inhibitors Mitigate N<sub>2</sub>O Losses in a Soil Cropped With Winter Wheat. *Nutr. Cycling Agroecosyst.* **2022**, *123*, 119–135.
- (62) Kowalchuk, G. A.; Stephen, J. R. Ammonia-Oxidizing Bacteria: A Model for Molecular Microbial Ecology. *Annu. Rev. Microbiol.* **2001**, *55*, 485–529.
- (63) Roy, J.; Reichel, R.; Brüggemann, N.; Hempel, S.; Rillig, M. C. Succession of Arbuscular Mycorrhizal Fungi Along a 52-Year Agricultural Recultivation Chronosequence. *FEMS Microbiol. Ecol.* **2017**, *93*, fix102.
- (64) Nii-Anngang, S.; Grünewald, H.; Freese, D.; Hüttl, R. F.; Dilly, O. Microbial Activity, Organic C Accumulation and <sup>13</sup>C Abundance in Soils Under Alley Cropping Systems After 9 Years of Recultivation of Quaternary Deposits. *Biol. Fertil. Soils* **2009**, *45*, 531–538.
- (65) Zhao, Y.; Reichel, R.; Herbst, M.; Sun, Y.; Brüggemann, N.; Mörchen, R.; Welp, G.; Meng, F.; Bol, R. Declining Total Carbon Stocks in Carbonate-Containing Agricultural Soils Over a 62-Year

Recultivation Chronosequence Under Humid Conditions. *Geoderma* **2022**, *425*, 116060.

(66) Baier, C.; Modersohn, A.; Jalowy, F.; Glaser, B.; Gross, A. Effects of Recultivation on Soil Organic Carbon Sequestration in Abandoned Coal Mining Sites: A Meta-Analysis. *Sci. Rep.* **2022**, *12*, 20090.

(67) Chen, Q.; Qi, L.; Bi, Q.; Dai, P.; Sun, D.; Sun, C.; Liu, W.; Lu, L.; Ni, W.; Lin, X. Comparative Effects of 3,4-Dimethylpyrazole Phosphate (DMPP) and Dicyandiamide (DCD) on Ammonia-Oxidizing Bacteria and Archaea in a Vegetable Soil. *Appl. Microbiol. Biotechnol.* **2015**, *99*, 477–487.

(68) Bachtsevani, E.; Papazlatani, C. V.; Rousidou, C.; Lampronikou, E.; Menkissoglu-Spiroudi, U.; Nicol, G. W.; Karpouzas, D. G.; Papadopoulou, E. S. Effects of the Nitrification inhibitor 3,4-Dimethylpyrazole phosphate (DMPP) on the Activity and Diversity of the Soil Microbial Community Under Contrasting Soil pH. *Biol. Fertil. Soils* **2021**, *57*, 1117–1135.

(69) Castellano-Hinojosa, A.; González-López, J.; Vallejo, A.; Bedmar, E. J. Effect of Urease and Nitrification Inhibitors on Ammonia Volatilization and Abundance of N-Cycling Genes in an Agricultural Soil. *J. Plant Nutr. Soil Sci.* **2020**, *183*, 99–109.

(70) Zhang, L. M.; Hu, H.-W.; Shen, J. P.; He, J.-Z. Ammonia-Oxidizing Archaea Have More Important Role Than Ammonia-Oxidizing Bacteria in Ammonia Oxidation of Strongly Acidic Soils. *ISME J.* **2012**, *6*, 1032–1045.